

Combined Use of Cosurfactant/Surfactant Mixtures and Swelling Agents in the Synthesis of Mesoporous Titanium Oxophosphates

T. Czurylszkiewicz,[†] F. Kleitz,^{‡,§} F. Schüth,[‡] and M. Lindén^{*,†,‡}

Department of Physical Chemistry, Åbo Akademi University, Porthansgatan 3-5,
FIN-20500 Turku, Finland, and Max Planck Institut für Kohlenforschung,
Kaiser-Wilhelm-Platz 1, 45470 Mülheim an der Ruhr, Germany

Received August 19, 2002. Revised Manuscript Received June 13, 2003

In this contribution we present results connected to the successful use of a hydrophobic swelling agent, trimethylbenzene, in the synthesis of hexagonally ordered surfactant–titanium oxophosphate mesophases in the presence of a cationic surfactant under acidic conditions. Furthermore, when a nonionic cosurfactant was used together with the cationic surfactant, an efficient swelling was achieved. This effect is attributed to a decrease in the preferential interfacial curvature of the mixed cosurfactant/surfactant supramolecular aggregates. Removal of the surfactant from the titanium oxophosphate by calcination was successfully achieved and truly mesoporous materials were obtained. The materials were characterized by powder XRD, nitrogen sorption, TEM, and TG-DTA/MS.

Introduction

The finding that supramolecular assemblies of amphiphilic molecules can be used as structure-directing agents in the synthesis of mesoscopically ordered silica^{1,2} has given rise to a rapidly developing area of research in the field of organized matter.³ The synthesis strategy was soon extended to non-siliceous materials, the synthesis and applications of which have recently been reviewed by Schüth.⁴ However, although removal of the template without structural collapse of the inorganic network is quite straightforward for siliceous materials, it is a much more difficult task for transition metal oxides.^{5,6} One of the reasons for this is the high reactivity of the precursors, typically alkoxides, and their tendency to form structures with a high degree of

internal condensation,⁷ but with a lower degree of condensation between the subunits building up the inorganic framework.⁸ Despite the well documented possibilities for tuning the pore size of siliceous mesoporous materials, for example by the solubilization of hydrophobic swelling agents inside the supramolecular surfactant aggregates (see for example ref 2), pore size engineering for ordered, non-siliceous materials has mainly been limited to the use of surfactants of different chain length. However, there is no fundamental reason that other approaches, which work for silica, could not be extended to non-siliceous materials. Because of the vast potential applications in fields such as chemical sensing, photocatalysis, and optics, the synthesis of mesoscopically ordered titania,^{9–14} titanium phosphate,¹⁵ titanium oxosulfate,¹⁶ titanium oxophosphate,^{17,18} and titanium fluorophosphate¹⁹ has attracted a lot of interest. We therefore chose a previously published synthesis protocol resulting in ordered microporous-

* To whom correspondence should be addressed. E-mail: mlinden@abo.fi.

[†] Åbo Akademi University.

[‡] Max Planck Institut für Kohlenforschung.

[§] Present address: Center for Functional Nanomaterials, Korea Advanced Institute of Science and Technology, Daejeon, South Korea.

(1) Kresge, C. T.; Leonowicz, M. E.; Roth, W. J.; Vartuli, J. C.; Beck, J. S. *Nature* **1992**, *359*, 710.

(2) Beck, J. S.; Vartuli, J. C.; Roth, W. J.; Leonowicz, M. E.; Kresge, C. T.; Schmitt, K. D.; Chu, C. T.-W.; Olson, D. H.; Sheppard, E. W.; McCullen, S. B.; Higgins, J. B.; Schenkler, J. L. *J. Am. Chem. Soc.* **1992**, *114*, 10834.

(3) For recent reviews see (a) Patarin, J.; Lebeau, B.; Zana, R. *Curr. Opin. Colloid Interface Sci.* **2002**, *7*, 107. (b) Ying, J. Y.; Mehnert, C. P.; Wong, M. S. *Angew. Chem., Int. Ed.* **1999**, *38*, 56. (c) Barton, T. J.; Bull, L. M.; Klemperer, W. G.; Loy, D. A.; McEnaney, B.; Misono, M.; Monson, P. A.; Pez, G.; Scherer, G. W.; Vartuli, J. C.; Yaghi, O. M. *Chem. Mater.* **1999**, *11*, 2633. (d) Ciesla, U.; Schüth, F. *Microporous Mesoporous Mater.* **1999**, *27*, 131. (e) Lindén, M.; Schacht, S.; Schüth, F.; Steele, A.; Unger, K. K. *J. Porous Mater.* **1998**, *5*, 177. (f) Zhao, D.; Yang, P.; Huo, Q.; Chmelka, B. F.; Stucky, G. D. *Curr. Opin. Solid State Mater. Sci.* **1998**, *3*, 111.

(4) Schüth, F. *Chem. Mater.* **2001**, *13*, 3184.

(5) Huo, Q.; Margolese, D.; Ciesla, U.; Feng, P.; Gier, T.; Sieger, P.; Firouzi, A.; Chmelka, B. F.; Schüth, F.; Stucky, G. D. *Nature* **1994**, *368*, 317.

(6) Ciesla, U.; Demuth, D.; Leon, R.; Petroff, P. M.; Stucky, G. D.; Unger, K. K.; Schüth, F. *J. Chem. Soc., Chem. Commun.* **1994**, 1387.

(7) Blanchard, J.; Ribot, F.; Sanchez, C.; Bellot, P. V.; Trokiner, A. *J. Non-Cryst. Solids* **2000**, *265*, 83.

(8) Solier-Illia, G. J. de A. A.; Scolan, E.; Louis, A.; Albouy, P.-A.; Sanchez, C. *New J. Chem.* **2001**, *25*, 156.

(9) Antonelli, D. M.; Ying, J. Y. *Angew. Chem., Int. Ed. Engl.* **1995**, *34*, 2014.

(10) Yang, P.; Xiao, D.; Margolese, D. I.; Chmelka, B. F.; Stucky, G. D. *Chem. Mater.* **1999**, *11*, 2813.

(11) Trong On, D. *Langmuir* **1999**, *15*, 8561.

(12) Cabrera, S.; El Haskouri, J.; Beltrán-Porter, A.; Beltrán-Porter, D.; Marcos, M. D.; Amorós, P. *Solid State Sci.* **2000**, *2*, 513.

(13) Solier-Illia, G. J. de A. A.; Louis, A.; Sanchez, C. *Chem. Mater.* **2002**, *14*, 750.

(14) Khushalani, D.; Dag, Ö.; Ozin, G. A.; Kuperman, A. *J. Mater. Chem.* **1999**, *9*, 1491.

(15) Bhaumik, A.; Inagaki, S. *J. Am. Chem. Soc.* **2001**, *123*, 691.

(16) Lindén, M.; Blanchard, J.; Schacht, S.; Schunk, S. A.; Schüth, F. *Chem. Mater.* **1999**, *11*, 3002.

(17) Thieme, M.; Schüth, F. *Microporous Mesoporous Mater.* **1999**, *27*, 193.

(18) Blanchard, J.; Schüth, F.; Trens, P.; Hudson, M. *Microporous Mesoporous Mater.* **2000**, *39*, 163.

(19) Serre, C.; Hervieu, M.; Magnier, C.; Taulelle, F.; Férey, G. *Chem. Mater.* **2002**, *14*, 180.

titanium oxophosphate¹⁸ to investigate the possibility of increasing the pore size to the mesopore-range by solubilization of a hydrophobic additive inside the organic portion of the mesophase. The aqueous synthesis is based on the utilization of titanium isopropoxide, sulfuric acid, and the structure-directing agent alkyltrimethylammonium bromide. Being a strongly complexing group, the sulfate coordinates to the titanium oxo-hydroxo-polymers formed immediately upon contact with water and renders them negatively charged. The inorganic-surfactant interaction is of electrostatic nature and occurs between negatively charged sulfate groups of the transition metal poly-ions and the positively charged surfactant. Successful removal of the surfactant is possible only if the sulfate groups are exchanged for more thermally stable phosphate groups by postsynthesis treatment.^{17,18,20} In addition to the use of a swelling agent, we also explore a mixed template approach, as we have previously shown that the use of a cosurfactant is an efficient means of affecting the preferential interfacial curvature of ordered organic-inorganic mesophases and therefore enhancing the solubilization capacity.^{21,22} The as-synthesized materials have been characterized by powder X-ray diffraction (XRD/SAXS) and thermogravimetry-differential thermal analysis coupled with mass spectrometry (TG-DTA/MS). Calcined and dried materials have been characterized by XRD, N₂ sorption, and transmission electron microscopy (TEM).

Experimental Section

Reagents. Hexadecyltrimethylammonium bromide (CTAB, Aldrich), 1,3,5-trimethylbenzene (TMB, Merck), 1-octanol (Fluka), titanium isopropoxide, Ti(OPrⁱ)₄, Merck, phosphoric acid 85% (Merck), and sulfuric acid 96% (J. T. Baker) were used as received without further purification.

Titanium Oxophosphate. The synthesis is derived from the procedure described by Blanchard et al.¹⁸ Titanium isopropoxide, Ti(OPrⁱ)₄ ($2.2 \cdot 10^{-2}$ mol), was dissolved in 70 mL of H₂SO₄ 0.5 M to which 90 mL of water containing $6.6 \cdot 10^{-3}$ mol of hexadecyltrimethylammoniumbromide, CTAB, was added, yielding a total molar composition of CTAB/H₂O/H₂SO₄/(TiOPrⁱ)₄ = 0.3/400/1.6/1. The procedure was modified by the addition of trimethylbenzene, TMB, and 1-octanol. The additives were added to the CTAB solution in $n_{\text{TMB}}/n_{\text{CTAB}}$ ratios (o) of 1, 2, 3, and 4, and $n_{1\text{-octanol}}/n_{\text{CTAB}}$ ratios (m) of 0.048, 0.096, and 0.144. A stirring rate of 500 rpm was used, if not otherwise mentioned, and the synthesis temperature was 30 °C. To achieve a thermally stable material the as-synthesized, filtered, and washed powders were aged under stirring for 8 h in a 0.5 M aqueous solution of phosphoric acid. The samples were then filtered and dried overnight at 90 °C. The samples were typically calcined according to 3 different protocols. Protocol 1: 1 h at 250 °C, 3 h at 350 °C; Protocol 2: 1 h at 250 °C, 2 h at 350 °C, 1 h at 400 °C; Protocol 3: 2 h at 250 °C, 2 h at 350 °C, and 2 h at 450 °C. All calcinations were performed under air with a heating rate of 0.5 °C/min.

Analysis. Small-angle X-ray scattering (SAXS) measurements were performed on a Kratky compact small-angle system, with a Seifert ID-3003 X-ray generator providing Cu K α radiation of wavelength 1.542 Å and a position sensitive detector, consisting of 1024 channels. To minimize the back-

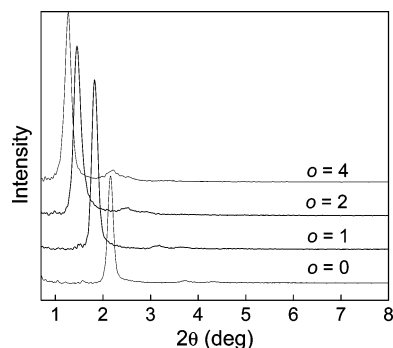


Figure 1. XRD diffractograms of as-synthesized titanium oxophosphate at different values of $o = n_{\text{TMB}}/n_{\text{CTAB}}$.

ground scattering from air, the camera volume was kept under vacuum during the measurements. The measurements were performed on wet samples before the drying step and on calcined samples. X-ray diffraction patterns were recorded in the range of 0.2–9° (2θ) with step 0.01° (2θ) and total time of 600 s.

Alternatively, calcined samples were analyzed with a Stoe STADI P diffractometer equipped with a linear position sensitive detector in transmission geometry using Cu K α_1 radiation. XRD patterns were recorded in the ranges of 1–10° (2θ) with step = 0.5° (2θ), and time/step = 60 s. Samples were additionally analyzed on a Stoe STADI P θ – θ powder X-ray diffractometer in reflection geometry (Bragg–Brentano) using Cu K α_{1+2} radiation with secondary monochromator and a scintillation detector. XRD patterns were recorded in the ranges of 1–10° (2θ) with step = 0.05° (2θ), and time/step = 20 s.

The thermogravimetric analyses combined with differential thermal analyses were performed on a Netzsch STA 449 C thermobalance coupled with a Balzers Thermostat 442 mass spectrometer (temperature of the transfer capillary 160 °C). The measurements were carried out under air with a heating rate of 5 °C/min for dried as-synthesized samples prior to template removal, and with a heating rate of 20 °C/min for calcined samples. All TG-DTA and MS results are reproducible within an error estimated to be ± 10 °C.

N₂ sorption measurements were performed at 77 K on an ASAP 2010 (Micromeritics). Prior to the measurement, the calcined samples were activated under vacuum for 5 h at 150 °C.

Transmission electron micrographs of the mesoporous titanium oxophosphate samples were obtained with a Hitachi HF 2000 transmission electron microscope operated at 200 keV, which was equipped with a cold field emission source. Calcined samples were mounted on carbon films that were fixed on copper grids.

Results and Discussion

As-Synthesized Materials. Formation of the hexagonal titania mesophase in this specific synthesis is very rapid, and a white precipitate is immediately formed upon mixing the aqueous solution of CTAB with the inorganic precursor solution. When the synthesis is carried out in the presence of TMB, a continuous increase in the d spacing of the hexagonal mesophase is observed with an increasing $n_{\text{TMB}}/n_{\text{CTAB}}$ molar ratio, o , as shown in Figure 1. The (100) reflection remains narrow and the (110) and (200) reflections, which are characteristic for a two-dimensional hexagonal phase, are clearly visible for $o \leq 4$, suggesting that the materials still possesses a high degree of structural order. For $o = 4$ the unit cell parameter a is 7.8 nm, which is substantially larger than $a = 4.8$ nm observed for $o = 0$. The result obtained for $o = 0$ is in good

(20) Kleitz, F.; Schmidt, W.; Schüth, F. *Microporous Mesoporous Mater.* **2001**, 44–45, 95.

(21) Kleitz, F.; Blanchard, J.; Zibrowius, B.; Schüth, F.; Ågren, P.; Lindén, M. *Langmuir* **2002**, 18, 4963.

(22) Lind, A.; Andersson, J.; Karlsson, S.; Ågren, P.; Bussian, P.; Amenitsch, H.; Lindén, M. *Langmuir* **2002**, 18, 1380.

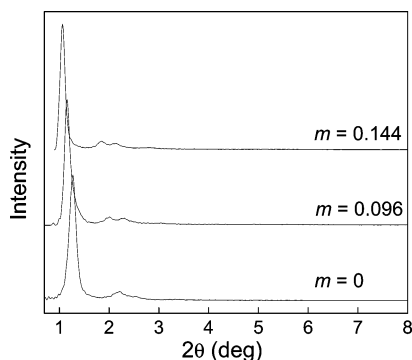


Figure 2. XRD diffractograms of as-synthesized titanium oxophosphate synthesized at a constant o value of 4; $m = 0$, 0.096, and 0.144, respectively.

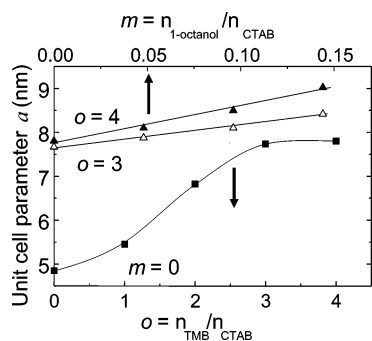


Figure 3. Dependency of the unit cell parameter of the hexagonal titanium oxophosphate phase, a , on o (bottom x -axis) and m at constant indicated values of o (top x -axis).

agreement with the work of Blanchard et al.¹⁸ The degree of swelling observed in the presence of TMB is slightly dependent on the stirring rate, with the $d(100)$ value increasing by 0.75 nm when the stirring rate is increased from 200 to 500 rpm at $o = 3$, which highlights the role of long-range hydrodynamic effects in the synthesis.²³ Furthermore, when the stirring rate is further increased to 600 rpm, a mixture of a hexagonal and a lamellar phase is generally observed. All results presented in the following were obtained at a constant stirring rate of 500 rpm, which turns out to be the optimum condition. Similar syntheses were carried out using 1-octanol as cosurfactant. The corresponding X-ray diffractograms, shown in Figure 2, indicate that the resulting materials conserved a very high degree of order. Keeping the o value constant at 3 or 4, a continuous increase in the d_{100} -spacing of the hexagonal mesophase is observed with increasing $n_{1\text{-octanol}}/n_{\text{CTAB}}$ molar ratio, m , as shown in Figure 3, reaching a maximum of 9.1 nm for $o = 4$ and $m = 0.14$. However, a further increase in m leads to the formation of a poorly ordered material with a coexisting lamellar phase.

These results clearly indicate the potential of the use of mixed surfactant templates together with a swelling agent for the synthesis of large pore mesoscopic materials. Alternatively, syntheses in which 1-octanol was replaced by an equal molar amount of CTAB did not result in an increase in the unit cell parameter of the titania materials. This finding shows that 1-octanol facilitates the formation of a supramolecular assembly with a lower interfacial curvature, which is needed for

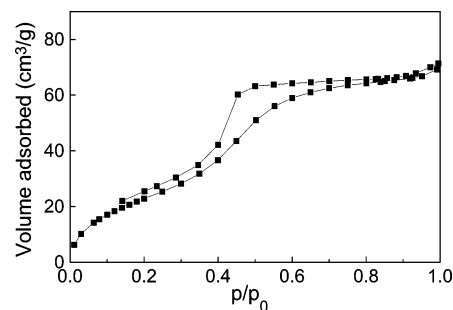


Figure 4. Nitrogen-sorption isotherm of titanium oxophosphate, $o = 4$ and $m = 0.096$, dried at 90 °C for 17 h. The sample was evacuated for 6 h at 150 °C prior to the measurement.

an enhanced solubilization of TMB. Formation of the inorganic-surfactant mesophase occurs immediately upon mixing of the reagents due to the presence of transition metal poly-ions in solution. The large size of the inorganic poly-ions decreases the interfacial flexibility of the composite mesophase, limiting its solubilization capacity. Therefore the locus of solubilization of the swelling agent in the initially formed surfactant micelles is crucial for the performance of the swelling agent in these rapidly precipitating systems.

Ordered inorganic-surfactant mesophases can therefore be synthesized in a fairly straightforward manner by the right choice of swelling agent and cosurfactant. Proof for the swelling action of the TMB are the mesoporous materials obtained if TMB is evaporated from the as-synthesized CTAB-titania mesophase upon heating at 90 °C for 17 h and further during activation of the sample before performing the sorption measurements. The corresponding N_2 -isotherm for such a material is shown in Figure 4. The pore size peaks at 3.2 nm ($BJH_{\text{desorption}}$) due to instability of the meniscus, but although the adsorption branch is quite steep around p/p_0 0.45, the pronounced H2 type hysteresis loop indicates that the pore surface may be corrugated. The fact that the adsorption and desorption branch do not meet at lower pressures is attributed to entrapment of N_2 molecules between the surfactant chains.²⁴ Because the surfactant is still cladding the wall, this is a simple approach to prepare hydrophobically modified, mesoporous titania.

Calcined Mesoporous Materials. Details of the processes involved in removal of the template from transition metal-based oxophosphate materials have been characterized previously.²⁰ These investigations have shown that removal of cationic surfactants from the titanium oxophosphate mesophase occurs via an oxidation reaction of the alkylammonium template accompanied by an exothermic effect with high energy release at temperatures around 290 °C. During this step, about 50% of the organic portion is removed. The residual organics are converted into carbonaceous species that are usually removed by heating at higher temperatures. However, the presence and nature of residual coke within the porous network of titanium oxophosphate are dependent on the thermal treatment applied to the material after synthesis. In addition, the properties of the final materials are severely altered by

(23) Schacht, S.; Huo, Q.; Voigt-Martin, I. G.; Stucky, G. D.; Schüth, F. *Science* **1996**, 273, 768.

(24) Keene, M. T. J.; Gougeon, R. D. M.; Denoyel, R.; Harris, R. K.; Rouquerol, J.; Llewellyn, P. L. *J. Mater. Chem.* **1999**, 9, 2843.

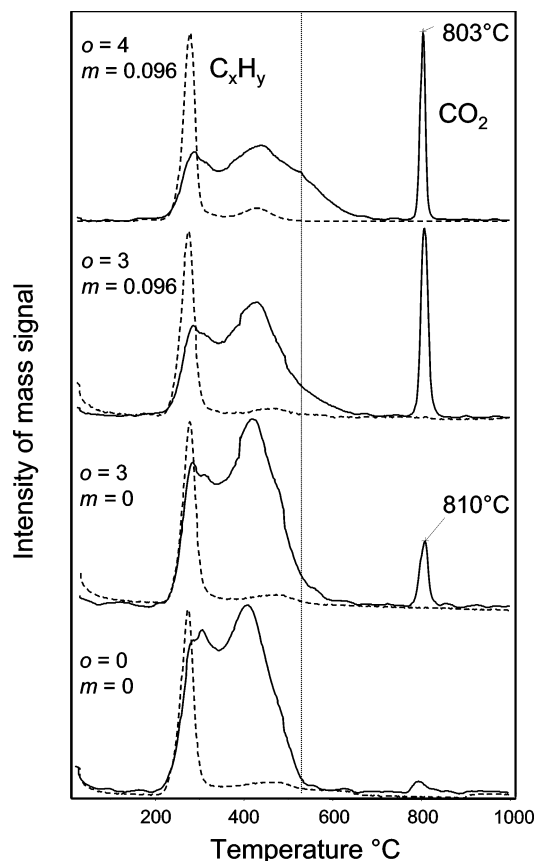


Figure 5. MS plots with temperature of titanium oxophosphate materials synthesized with the indicated o and m values, obtained by TG-DTA/MS.

Table 1. Weight Losses (%) Measured by TG for Titanium Oxophosphate Samples Synthesized with Different Amounts of Additional Organics (Heating Ramp: 5 °C/min under Air)

[TMB]/ [OcOH]/[CTAB]	30–180 °C	180–330 °C	330–550 °C	550–1000 °C
0/0/1	6	18	26	0.5
3/0/1	5	17	27	2
3/0.096/1	5	16	24	5
4/0.096/1	5	16	23	6

high-temperature treatments.^{20,25} In the case of the truly mesoporous titania-based mesophases described herein, the solids contain a substantial amount of additional organic species, which may drastically alter, or even hinder, the processes of thermodesorption and degradation of the template. To analyze the thermal behavior of the mixed organic/surfactant inorganic composites, we have therefore carried out TG-DTA experiments coupled with MS on samples synthesized in the presence of different amounts of organic additives. The results of the TG investigations are summarized in Table 1. After removal of the physisorbed water below 180 °C, three main steps are observed in the weight loss. All observed steps in the mass-loss curve are assigned to exothermic processes, and correspond to the degradation of the templating species and combustion reactions. When no TMB was added to the synthesis, the last step was negligible. An increase in the weight loss at high temperatures is observed with increasing amount of additional organics. On the other hand, the proportion

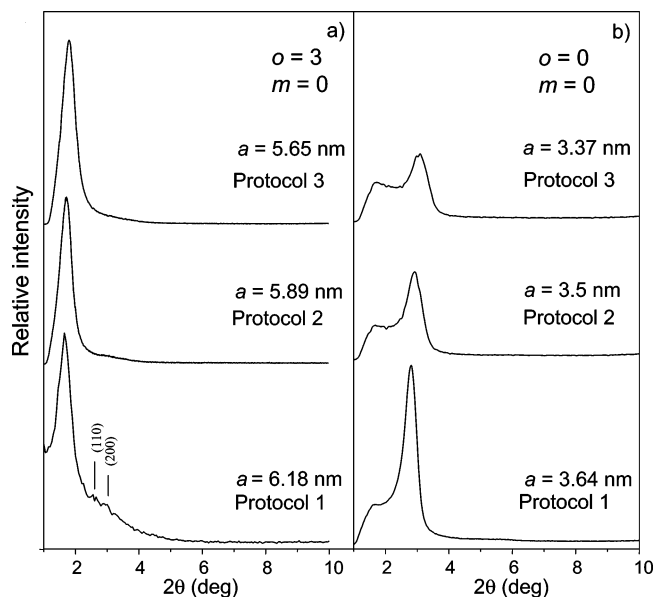


Figure 6. XRD-diffractograms of calcined titanium oxophosphate $o = 3$, $m = 0$ (a) and $o = 0$, $m = 0$ (b) calcined according to three different calcination protocols: (1) 1 h at 250 °C, 3 h at 350 °C; (2) 1 h at 250 °C, 2 h at 350 °C, 1 h at 400 °C; and (3) 2 h each at 250 °C, 350 °C, and 450 °C.

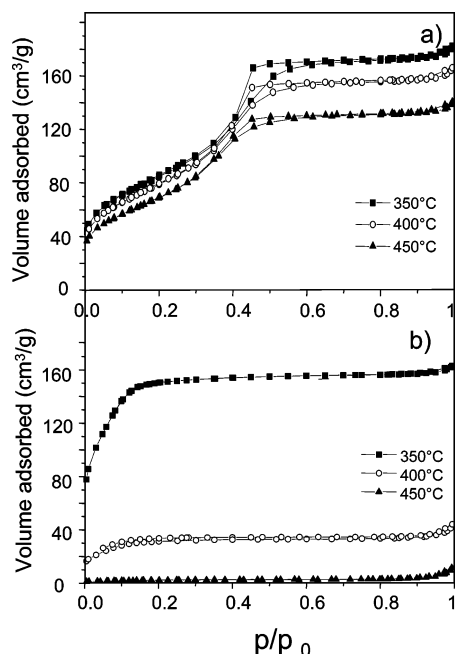
of leaving species at lower temperature seems to decrease. The curves recorded from the MS (Figure 5) allow characterization of the species evolved at the different temperature steps. The representative curves show the evolution of molecular species assigned to CO_2 ($m/z = 44$) with a dotted line and C_xH_y ($m/z = 41, 42, 59, 75$) with a solid line, as a function of temperature for different initial amounts of additives. The curves corresponding to hydrocarbon species are similar in all cases, with the peak maximum centered at 277 °C. However, with increasing amounts of additives, CO_2 is released at temperatures up to 650 °C. A subsequent peak detected at about 810 °C in the CO_2 trace becomes more pronounced with increasing initial amount of organic additives. In agreement with the thermogravimetric data, this suggests that increasing amounts of residual carbonaceous species are retained in the materials after combustion of the templating mixture for the samples synthesized in the presence of swelling agents. Controlled calcination protocols with slow heating rates may allow the use of higher temperature for the thermal treatment, which could be more favorable for coke removal. In attempts to reduce the damage caused by the combustion of the template and rapid local overheating, isothermal steps (plateaus) were introduced during the heating ramp of the calcination protocol, at the temperatures where structural and thermal events take place.²⁰ Three different calcination protocols under air were tested (see Experimental Section for details).

Figure 6a) shows the XRD patterns obtained after calcination according to the different protocols tested. This material exhibits a unit cell with $a = 7.8$ nm before calcination. The XRD results suggest that the ordered hexagonal structure was retained after the template removal. However, a strong shift of the d spacing toward lower values is observed for all calcination protocols. Blanchard et al.¹⁸ observed a substantial framework contraction of about 33% for titanium oxophosphate

Table 2. Physicochemical Parameters Obtained by XRD and Nitrogen Physisorption for Titanium Oxophosphate Synthesized at Different TMB/OcOH/CTAB Ratios

calcination protocol	[TMB]/[OcOH]/[CTAB]	unit cell a (nm)	pore volume, V_p (cm ³ /g)	BET surface area (m ² /g)	pore diameter BJH des. (nm)	pore diameter w_d ^b (nm)
1	3/0/1	6.18 (3.6) ^a	0.25 (0.24) ^a	309	3.08	4.25
2	3/0/1	5.89 (3.4)	0.23 (0.05)	293	3.02	3.95
3	3/0/1	5.66 (3.3)	0.20 (0.01)	253	2.89	3.64
3	3/0.096/1	6.10 (3.3) ^a	0.25 (0.01)	268	3.33	4.20
3	4/0.096/1	6.41 (3.3)	0.30 (0.01)	290	3.22	4.63

^a Values in parentheses are for the non-swollen standard titanium oxophosphate (0/0/1). ^b Obtained from the geometrical model with equation $w_d = cd_{100} \cdot (V_p \rho / (1 + V_p \rho))^{1/2}$ where $c = 1.213$ (circular cylinders), $\rho = 3$ g/cm³, and V_p = pore volume.

**Figure 7.** Nitrogen-sorption isotherms of titanium oxophosphate (a) $o = 3$ and (b) with $o = 0$, calcined according to three different calcination protocols (Figure 6).

synthesized in the absence of swelling agent and calcined at 350 °C. In our case, a maximum contraction of 28% is measured when the calcination is carried out up to 450 °C. The material calcined at a temperature of 350 °C exhibits an XRD pattern with the presence of several low angle reflections, with a lattice constant of $a = 6.18$ nm, which represents a shrinkage of 21%. Increasing the calcination temperature resulted in a more pronounced shrinkage. No wide-angle reflections are observed excluding the presence of crystalline titania phases. For comparison, the standard material with no swelling agent was calcined according to the same protocols. The XRD patterns depicted in Figure 6b highlight the pronounced shrinkage and the dramatic loss of order observed already for low calcination temperatures. At 450 °C the structure fully collapses.

The results of the nitrogen physisorption measurements performed on the same samples are shown in Figure 7a and b. The materials synthesized in the presence of TMB show typical type IV sorption isotherms with an H2 type hysteresis loop, with decreasing adsorption capacity when the calcination temperature was increased (Figure 7a). The adsorption and desorption steps in the isotherm at relative pressures corresponding to mesopores in the 3–4 nm diameter range are quite steep, which can be taken as an indication for a narrow pore size distribution. Figure 7b shows the corresponding sorption isotherms for materials synthe-

Table 3. Weight Losses (%) Measured Above 300 °C for Different Calcination Protocols^a

calcination protocol	[TMB]/[OcOH]/[CTAB]			
	0/0/1	3/0/1	3/0.096/1	4/0.1/1
1	7	10	^b	16
2	3	5	^b	^b
3	1.5	2	3	^b

^a The weight changes are attributed to the elimination of residual carbonaceous species and water produced from hydroxyl condensation at high temperature. ^b Not measured.

sized without any swelling agent, with the adsorption isotherms being of Type 1 indicating microporosity. Rapid collapse of the mesostructure is observed with increasing calcination temperature. However, these materials still showed an increased adsorption capacity compared to materials calcined following the previously described protocols.¹⁸ Some physicochemical parameters of the materials obtained according to the different calcination protocols are listed in Table 2. The BJH desorption pore diameters are given together with the pore diameter estimated on the basis of the geometrical model proposed by Kruk et al.²⁶ Surface areas as high as 300 m²/g could be obtained when $o = 3$ and $m = 0$. However, a decrease in both pore size and surface area is observed with increasing calcination temperature. On the basis of the values of a and the corresponding pore diameter one can conclude that the pore wall thickness is about 2 nm regardless of the calcination protocol applied. The TMB and 1-octanol containing titanium oxophosphates with $o = 3$, $m = 0.096$, and $o = 4$, $m = 0.096$, also show a typical type IV isotherm indicative of mesoporosity, similar to the isotherms presented in Figure 7a. The BET surface areas of the corresponding materials are 270 m²/g and 290 m²/g, and the calculated pore sizes are found in Table 3. Furthermore, the pore size distribution is shown to be relatively narrow, with pore diameters around 4 nm for samples with $o = 3$, and $m = 0$, and around 4.5 nm for samples with $o = 3$ or 4, and $m = 0.096$. A TEM image of a titanium oxophosphate sample obtained after calcination is shown in Figure 8. It is evident that the hexagonal structure is retained after calcination. Furthermore, no regions containing bulk-crystalline titania could be found. From these results, it is clear that the titanium oxophosphates obtained exhibit true mesoporosity and a thermal stability significantly higher than that of standard materials. The higher thermal stability may originate from both a stabilizing effect of coke remaining in the samples after calcination, as also indicated for mesostructured aluminosilicate materials with zeolitic walls,²⁷ and from the increased separation of the phosphate

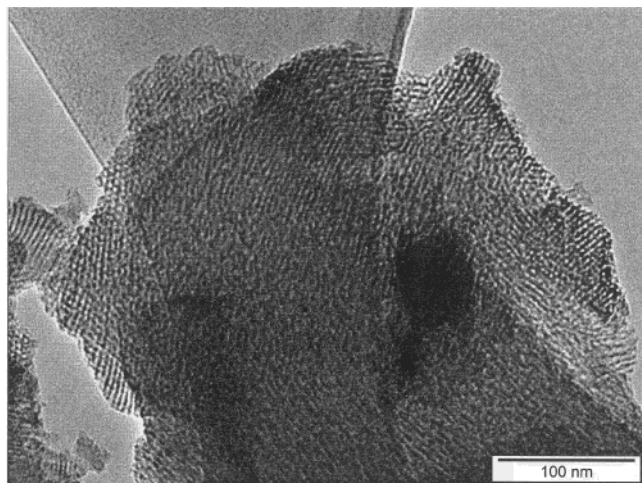


Figure 8. TEM image of a titanium oxophosphate material ($o = 3$, $m = 0$) calcined according to protocol 3.

surface-groups for the materials with larger pores. Furthermore, the lower curvature of the walls could lead to decreased strain and thus make the material more stable. In addition, it is known that the deterioration of the material starts at the pore mouth, which could make them inaccessible to nitrogen, while the internal channel system still remains intact.^{18,20} If the pores are bigger to begin with, small changes at the pore mouth still leave the pore system accessible and nitrogen sorption capacity is maintained. In general, the different calcined samples studied show relatively good adsorp-

tion properties, and the long-range order of the materials was conserved. However, the materials show different colorations after calcination, attributed to the presence of residual coke in the materials.

Conclusions

Pore size enlargement of mesoscopically ordered titanium oxophosphate has been performed by solubilizing a hydrophobic swelling agent inside the surfactant part of the inorganic-organic mesophase during the synthesis. The unit cell parameter, a , could be successfully increased to 9.1 nm while still maintaining a high degree of long-range order in the as-synthesized material with a combination of TMB as the swelling agent and 1-octanol as a cosurfactant. Removal of the organic portion by calcination was possible without loss of the mesoscopic order at calcination temperatures less than 450 °C. However, residual carbonaceous species remained in the samples after calcination, which is a problem that remains to be solved. The calcined titanium oxophosphate materials showed a well-resolved hexagonal structure in the TEM images. The pore size expansion strategy demonstrated here is thought to be a general one and readily adaptable also for pore size enlargement of other non-siliceous materials.²⁸

Acknowledgment. Financial support from the Finnish Technology Center, TEKES, (T.C. and M.L.) and the European Union funded project HPRN-CT-1999-00025 (F.K. and F.S.) are gratefully acknowledged. We thank B. Spliethoff (MPI für Kohlenforschung, Mülheim) for the TEM images.

CM021293T

(27) Liu, Y.; Zhang, W.; Pinnavaia, T. J. *J. Am. Chem. Soc.* **2000**, *122*, 8791.

(28) Czurylszkiewicz, T.; Rosenholm, J.; Kleitz, F.; Lindén, M. *Stud. Surf. Sci. Catal.* **2002**, *142*, 1117.